Expanded Close-Packed Fullerides: The Reactivity of Na_2C_{60} with Ammonia

Amelia J. Fowkes, Judith M. Fox, Paul F. Henry, Stephen J. Heyes, and Matthew J. Rosseinsky*

Contribution from the Inorganic Chemistry Laboratory, University of Oxford, South Parks Road, Oxford OX1 3QR, U.K.

Received June 24, 1997[⊗]

Abstract: A novel expanded fulleride results from the room temperature reaction of Na_2C_{60} with ammonia. The rhombohedral packing of $(ND_3)_8Na_2C_{60}$ arises from cooperative rearrangement of the face-centered cubic structure of the starting material, via a bcc intermediate. The interfulleride distance within the formerly close-packed layers increases to 12.22 Å while 10.24 Å contacts are maintained between the layers, which retain an ABC stacking sequence. A combination of minimized C···D repulsions and attractive N−D···π interactions between the dynamically reorientating $Na(ND_3)_4^+$ and C_{60}^{2-} units control the structure.

Introduction

The organization of extended molecular arrays is related to the development of low-temperature synthetic strategies in which structural elements of the reagents are recognizable in the products.[1] In recent molecular solid state chemistry, the discovery of superconductivity in alkali metal fullerides is an important development. Here we show how fulleride packing can be modified by room temperature ligand complexation of the intercalated sodium cations in Na_2C_{60} and analyze the structural changes in terms of the close D···C contacts produced by formation of the complex cations. The motivation for the study is to extend the number of structure types in which 10 Å interfulleride contacts are maintained beyond the face-centered cubic (fcc)/body-centered cubic (bcc) packings accessible by higher temperature chemistry.

A rich variety of electronic properties, including superconductivity in A_3C_{60} compounds[2] and ferromagnetism,[3] have resulted from the relatively small number of well-characterized materials containing anions of the most abundant fullerene, C_{60}.[4,5] The highest superconducting transition temperature of 40 K is not found in the fcc structure, which is most common at the A_3C_{60} composition, but in bcc Cs_3C_{60}[6] where the fulleride anion has eight nearest neighbors at 10.0 Å. There is thus a need to develop chemical routes to fullerides with novel packings in which close contact is maintained between the fulleride anions, but the coordination number is reduced.

One method of achieving this is to use nonspherical molecular or complex counterions. In the primitive hexagonal tetramethylammonium fullerides,[7] close-packed C_{60}^{n-} ($n = 1, 2$) layers are stacked in an AAA sequence. Complexation of intercalated alkali metal cations with ammonia has afforded the expanded fcc array of $(NH_3)_4Na_2CsC_{60}$ from Na_2CsC_{60},[8] bcc $(NH_3)_6Na_3C_{60}$ from Na_3C_{60}[9] and body-centered tetragonal and orthorhombic packings,[10−12] but no new fulleride structure types have yet resulted from this approach. Understanding the chemical factors which control these packing motifs requires detailed information on the nonbonded contacts between the fulleride and the counterion.

Na_2C_{60} has an fcc structure with sodium on both tetrahedral sites.[13−15] Here we show that this compound reacts with ammonia to afford $(NH_3)_8Na_2C_{60}$, which adopts a novel structure. All the sodium cations are tetrahedrally coordinated by ammonia, and each C_{60}^{2-} has only six nearest fulleride neighbors at 10.244 Å separation in a rhombohedral packing. Using a combination of neutron and X-ray powder diffraction with multinuclear (^{13}C and ^{2}H) solid-state NMR, we explore the interaction between the positions and the dynamics of the fulleride anions and the complex countercations which produce the new packing arrangement. The structure type is inaccessible with higher temperature ($T \geq 300$ °C) chemistry and is seen to be controlled by the effect of the ammonia molecules on the $C_{60}-C_{60}$ separations within and between the close-packed layers.

Experimental Section

Synthesis of Starting Materials. C_{60} was prepared by spark erosion of graphite rods and purified by chromatography with a toluene eluent on Norit-Elorit carbon[16] followed by sublimation under dynamic vacuum (10^{-3} Torr) at 550 °C. Na_2C_{60} was prepared by reaction of

[⊗] Abstract published in *Advance ACS Abstracts,* October 1, 1997.

(1) Stein, A.; Keller, S. W.; Mallouk, T. E. *Science* **1993**, *259*, 1558.
(2) Hebard, A. F.; Rosseinsky, M. J.; Haddon, R. C.; Murphy, D. W.; Glarum, S. H.; Palstra, T. T. M.; Ramirez, A. P.; Kortan, A. R. *Nature* **1991**, *350*, 600.
(3) Allemand, P. M.; Khemani, K. C.; Koch, A.; Wudl, F.; Holczer, K.; Donovan, S.; Gruner, G.; Thompson, J. D. *Science* **1991**, *253*, 301.
(4) Rosseinsky, M. J. *J. Mater. Chem.* **1995**, *5*, 1497−1513.
(5) Fischer, J. E. *J. Phys. Chem. Solids.* In press.
(6) Palstra, T. T. M.; Zhou, O.; Iwasa, Y.; Sulewski, P. E.; Fleming, R. M.; Zegarski, B. R. *Solid State Commun.* **1995**, *93*, 327.
(7) Douthwaite, R. E.; Green, M. A.; Green, M. L. H.; Rosseinsky, M. J. *J. Mater. Chem.* **1996**, *6*, 1913.
(8) Zhou, O.; Fleming, R. M.; Murphy, D. W.; Rosseinsky, M. J.; van Dover, R. B.; Ramirez, A. P.; Haddon, R. C. *Nature* **1993**, *362*, 433.
(9) Henry, P. F.; Rosseinsky, M. J.; Watt, C. J. *J. Chem. Soc., Chem. Commun.* **1995**, 2131−2132.
(10) Rosseinsky, M. J.; Murphy, D. W.; Fleming, R. M.; Zhou, O. *Nature* **1993**, *364*, 425−427.
(11) Zhou, O.; Palstra, T. T. M.; Iwasa, Y.; Fleming, R. M.; Hebard, A. F.; Sulewski, P. E. *Phys. Rev. B* **1995**, *52*, 483.
(12) Fullagar, W. K.; Cookson, D.; Richardson, J. W., Jr.; Reynolds, P. A.; White, J. W. *Chem. Phys. Lett.* **1995**, *245*, 102.
(13) Rosseinsky, M. J.; Murphy, D. W.; Fleming, R. M.; Tycko, R.; Ramirez, A. P.; Siegrist, T.; Dabbagh, G.; Barrett, S. E. *Nature* **1992**, *356*, 416−418.
(14) Yildirim, T.; Fischer, J. E.; Harris, A. B.; Stephens, P. W.; Liu, D.; Brard, L.; Strongin, R. M.; Smith, A. B. *Phys. Rev. Lett.* **1993**, *71*, 1383−1386.
(15) Douthwaite, R. E.; Green, M. L. H.; Rosseinsky, M. J. *Chem. Mater.* **1996**, *8*, 394−400.
(16) Taylor, R.; Langley, G. J.; Kroto, H. W.; Walton, D. R. M. *Chem. Commun.* **1994**, 15.

S0002-7863(97)02085-4 CCC: $14.00

C_{60} with a stoichiometric quantity of sodium in a stainless steel tube sealed in a Pyrex tube (10^{-5} Torr). Reaction at 200 °C for 10 days to allow complete reaction of all the sodium metal was followed by an increase in temperature to 350 °C over 3 days. The sample was then ground and resealed and annealed at 450 °C for 7 days with three intermediate regrindings to homogenize the sodium concentration. This and all subsequent handling of air-sensitive reagents was performed in an Mbraun Labmaster drybox under a helium atmosphere. The progress of the reaction was monitored by powder X-ray diffraction and ^{13}C magic angle spinning (MAS) NMR.

Reaction of Na_2C_{60} with Ammonia. An accurately weighed aliquot of Na_2C_{60} (in the region of 100 mg, 0.13 mmol) was loaded in the drybox into an all-glass apparatus, which consisted of a reaction chamber containing the fulleride and a bulb to contain condensed NH_3. The bulb was loaded with an alkali metal filled capillary, the apparatus evacuated to 10^{-5} Torr, and ammonia condensed into the bulb from a reservoir ampule by using a slush bath at −78 °C. After 30 min, any noncondensable gas was pumped off, and the ammonia vapor pressure was controlled by changing the temperature of the surrounding bath from −43 °C (0.6 atm) to −107 °C (0.004 atm). The temperature of the Na_2C_{60} reagent was adjusted from room temperature to 100 °C. For quantitative measurement of the ammonia uptake, an electronic pressure transducer and a calibrated volume were added to the apparatus, and the ammonia pressure was adjusted by a pump-fill method after admission of dry NH_3. 53.7 mg (0.07 mmol) of Na_2C_{60} was used in these barometric measurements. The system was allowed to equilibrate for 20 min at each pressure during the measurement. The reaction apparatus contained 10 mmol of NH_3 gas at 0.6 atm.

Samples for X-ray diffraction and static NMR were prepared by loading the Na_2C_{60} reagent into capillaries or ampules blown on to the two-bulb apparatus. Post reaction, the samples were sealed under the ammonia pressure. Annealing experiments were conducted on the sealed ampules. Sample stability in the absence of an overpressure of ammonia was investigated by deammoniation at 300 °C under a dynamic vacuum, and by observing the effect on the X-ray powder diffraction pattern of leaving samples standing in the helium atmosphere of the drybox and in capillaries sealed under helium.

NMR. Measurements were carried out with a Bruker MSL200 spectrometer, operating at 50.32 MHz for ^{13}C. Samples for magic angle spinning (MAS)NMR were packed into 5-mm Kel-F capped inserts contained within 7 mm zirconia rotors with Kel-F caps. Samples for static NMR measurements were sealed in a 5 mm outer diameter 2 cm long Pyrex tube under either NH_3 or ND_3 (^{13}C or ^2H spectroscopy, respectively). ^2H quadrupole echo NMR spectra were measured over the range $150 \leq T/K \leq 370$, with a spin-echo delay of 30 μs and a recycle delay of 5 s. All ^2H NMR spectra were recorded on a Bruker MSL400 spectrometer with an Oxford Instruments 9.4 T wide bore superconducting solenoid magnet at 61.4 MHz using a Bruker HP-WB-73A CP-BB-VTM probe with a 7 mm horizontal coil. Temperature control was achieved with a Bruker B-VT1000 temperature control unit equipped with a copper−constantan thermocouple and digital reference. Temperatures were accurate to within ±1 K, and were stable to ±0.1 K. Twenty minutes were allowed for thermal equilibrium to be attained before spectral accumulation was commenced. The quadrupolar spin-echo technique[17] with standard precautions and phase cycling (to remove off-resonance effects)[18] was used for acquiring all ^2H NMR spectra. All spectra were recorded by using quadrature detection. Typically 3.5−4 μs 90° pulses and spin-echo times of 30−200 μs were employed. The recycle delay was 5 s. Sample integrity was confirmed after the NMR experiments by powder X-ray diffraction. Simulation of the ^2H NMR powder line shapes was performed with locally written FORTRAN programs,[19] based on the theory of Wittebort et al.[20]

Powder Diffraction. X-ray powder diffraction patterns were recorded in samples sealed in 0.7-mm capillaries under either helium or the vapor pressure of ammonia used in the experiment. Data were collected in 0.05° steps using a Siemens D5000 diffractometer with Cu Kα1 radiation from a Ge primary monochromator and a linear 6° position-sensitive detector. For powder neutron diffraction, 0.5 g of Na_2C_{60} was prepared as described above and reacted with aliquots of dry, deoxygenated ND_3 (K&K Greefe Ltd., 99+% isotopic purity), by successive 1 h exposures to 0.05 and 0.60 atm of ND_3, to produce an ammoniated phase of composition $(ND_3)_{7.9(5)}Na_2C_{60}$. The extent of reaction was monitored via the pressure change to ensure completion of the reaction. Exposure to 0.05 atm of ND_3 produced an intermediate uptake of 5.5(3) equiv of ammonia. The Pyrex ampule containing the reacted sample was then sealed. The sample was transferred rapidly in the drybox into a cylindrical vanadium can, which was sealed with indium wire. Powder neutron diffraction data were collected on the POLARIS diffractometer at the ISIS pulsed neutron source, Rutherford Appleton Laboratory at room temperature: a shorter dataset measured at 100 K indicated that no structural phase transition had occurred over the temperature range studied here. Rietveld refinement and Fourier analysis on both X-ray and neutron datasets were carried out on a 166-MHz Pentium PC with the GSAS suite of programs.[21] The X-ray data were collected in 0.05° steps over the angular range $8 \leq 2\theta/° \leq 80$ with a counting time of 100 s per step. A pseudo-Voigt peak shape function and a 30-term Chebyshev polynomial background function were employed. Neutron data from the C detector bank ($2\theta = 145°$, $\Delta d/d = 5 \times 10^{-3}$) over the d-spacing range $0.95 \leq d/Å \leq 3.2$ were refined. A pseudo-Voigt function peak shape convoluted with double-exponential decay, and an 18-term Chebyshev polynomial background function were employed for the neutron data. The relevant neutron scattering lengths are 0.665×10^{-12} cm for C, 0.667×10^{-12} cm for D, 0.930×10^{-12} cm for N, and 0.363×10^{-12} cm for Na. The refined parameters presented in Table 1 are the results of a combined refinement of the X-ray and neutron histograms.

Results

Pressure Dependence and Phase Formation. The 282 K ammonia uptake isotherm of Na_2C_{60} indicates a limiting uptake of 8 ammonia molecules per Na_2C_{60} formula unit at a pressure of 0.6 atm, with an initial rise to 5.3 equiv of ammonia at 0.05 atm. Reactions in sealed tubes indicate that the threshold pressure for the uptake of NH_3 by Na_2C_{60} lies between 0.007 atm (no reaction) and 0.01 atm at room temperature. Hysteresis occurs on the pressure-reduction leg of the isotherm, with the $n = 8$ phase formed at higher ammonia pressures being stable over the 20 min time scale of the measurements to a pressure of 0.01 atm.

X-ray powder diffraction shows that both the inflection in $n(P\{NH_3\})$ at $n = 5.3$ and the endpoint at $n = 8.00$ correspond to new phases. The most intense X-ray reflections of the $n = 5.3$ phase can be indexed by using the body-centered cubic cell found for $(NH_3)_6Na_3C_{60}$, with a larger lattice parameter of 12.169 Å. There are, however, several low-angle superlattice reflections. The structure of this phase, henceforth described as the bcc phase, will be described in a forthcoming publication.[22]

The higher pressure $n = 8$ phase has a new set of powder X-ray reflections and is not isostructural with any previously known fullerides. The powder diffraction pattern from this phase was indexed by using a hexagonal unit cell ($a = 12.221$ Å, $c = 22.296$ Å), with the systematic absences being consistent with rhombohedral space group symmetry. The crystallinity and diffraction pattern of the phase were not altered by annealing in sealed tubes at room temperature for up to 1 week, while higher temperature annealing produced increasing quantities of the bcc phase.

(17) Davis, J. H.; Jeffrey, K. R.; Bloom, M.; Valic, M. I.; Higgs, T. P. *Chem. Phys. Lett.* **1976**, *42*, 390.
(18) Bloom, M.; Davis, J. H.; Valic, M. I. *Can. J. Phys.* **1980**, *58*, 1510.
(19) Heyes, S. J.; Clayden, N. J.; Dobson, C. M. *J. Phys. Chem.* **1991**, *95*, 1547.
(20) Wittebort, R. J.; Olejniczak, E. T.; Griffin, R. G. *J. Chem. Phys.* **1987**, *86*, 5411.
(21) Larson, A. C.; von Dreele, R. B. *General Structure Analysis System*; Los Alamos National Laboratory, 1994.
(22) Fowkes, A. J.; Fox, J. M.; Henry, P. F.; Heyes, S. J.; Rosseinsky, M. J. In preparation.

Table 1. Refined Parameters[a] for $(ND_3)_8Na_2C_{60}$ at 298 K in Space Group $R\bar{3}m$ with the Unit Cell Parameters $a = 10.24325(13)$ Å, $\alpha = 73.2287(11)°$, and $V = 960.255(23)$ Å^3

Wyckoff position	site symmetry	atom	*x*	*y*	*z*	U_i/U_e (100 Å^2)	occupancy
6h	*m*	C1	0.22523(21)	0.22523(21)	−0.19731(32)	3.33(4)	1.00
12i	1	C2	0.36343(21)	−0.13204(21)	−0.01295(19)	3.33(4)	1.00
12i	1	C3	−0.26334(19)	−0.03122(18)	−0.14463(20)	3.33(4)	1.00
12i	1	C4	−0.24258(22)	−0.05108(21)	0.32647(22)	3.33(4)	1.00
6h	*m*	C5	0.19270(18)	0.19270(18)	−0.30407(29)	3.33(4)	1.00
12i	1	C6	0.31300(25)	−0.10939(23)	0.12150(21)	3.33(4)	1.00
6 h	*m*	N7	0.54793(27)	0.21202(38)	0.54793(27)	8.93*	1.00
12i	1	D8	0.6261(12)	0.1444(16)	0.5213(17)	14.81*	0.50
12i	1	D9	0.5563(10)	0.2203(16)	0.6327(10)	14.18*	0.50
12i	1	D10	0.4741(14)	0.1683(17)	0.5716(13)	17.21*	0.50
2c	3*m*	Na11	0.40981(23)	0.40981(23)	0.40981(23)	12.50(27)	1.00
2c	3*m*	N12	0.30262(28)	0.30262(28)	0.30262(28)	6.53(19)	1.00
12i	1	D13	0.3720(8)	0.2132(7)	0.2774(6)	8.68*	0.50

[a] Asterisks in the displacement parameter column indicate that the number quoted is the equivalent isotropic temperature factor for an atom refined anisotropically. It should be noted that while the structure is discussed in terms of the *R*-centered hexagonal cell, refinement was carried out in the primitive rhombohedral cell for technical reasons associated with the use of a rigid body for the equatorial ND_3 molecule. The refined parameters are presented for this cell.

The reactions to form either phase were complete within 30 min at room temperature. Ammonia uptake was found to be irreversible on this time scale. The rhombohedral high-pressure phase is formed smoothly by the sequential method of exposing the low-pressure bcc phase (formed at 0.05 atm) to 0.6 atm of NH_3. Direct exposure of Na_2C_{60} to 0.6 atm of NH_3 without formation of the bcc phases through previous exposure to lower ammonia pressure results in the formation of a very poorly crystalline product.

On standing open in the drybox, the rhombohedral $n = 8$ phase lost crystallinity over a period of 5 h, demonstrated by broadening of the X-ray Bragg reflections. We associate this with loss of ammonia, as the weight of the sample decreases slowly on the balance in the recirculating helium atmosphere of the drybox. On standing for a week in the drybox, and for several months in capillaries with 80% dead space, almost complete conversion to the bcc phase occurred through deammoniation. The $n = 5.3$ bcc phase, in contrast, appears stable to standing (for 3 months) in the absence of ammonia if water and dioxygen are rigorously excluded. Heating to 300 °C under dynamic vacuum leads to irreversible decomposition into C_{60} and sodium fullerides.

X-ray diffraction shows that the rhombohedral phase is able to accommodate variable ammonia concentrations. The rhombohedral phases present together with the bcc phase in both incompletely reacted and partially deammoniated samples have smaller cell volumes: the rhombohedral component of a sample prepared under 0.23 atm of ND_3 and annealed at room temperature for 5 days had a unit cell volume $V = 2865(1)$ Å^3 while the largest cell volume of 2885 Å^3 was found for a sample prepared under 0.6 atm and subsequently sealed under this pressure in a capillary.

^{13}C NMR Spectroscopy. ^{13}C NMR is a powerful probe for the identification of new C_{60}-containing phases.[23] The bcc phase $(NH_3)_{5.3}Na_2C_{60}$ is sufficiently stable to allow MASNMR measurement in a tightly-capped insert within a rotor, and gives rise to a single isotropic peak at 184(1) ppm, showing complete reaction of the Na_2C_{60} starting material. The more heavily loaded rhombohedral phase partially deammoniates under the MAS measurement conditions over the required acquisition time (250 scans, 20 s recycle delay). The wideline solid-state ^{13}C NMR spectrum of the sample sealed in a Pyrex tube under 0.32 atm of ND_3 was therefore measured. This gave a single resonance with an isotropic shift of 180(3) ppm (Figure 1). Both the ammoniated phases have resonances well-shifted from the 172 ppm[24] of the Na_2C_{60} starting material.

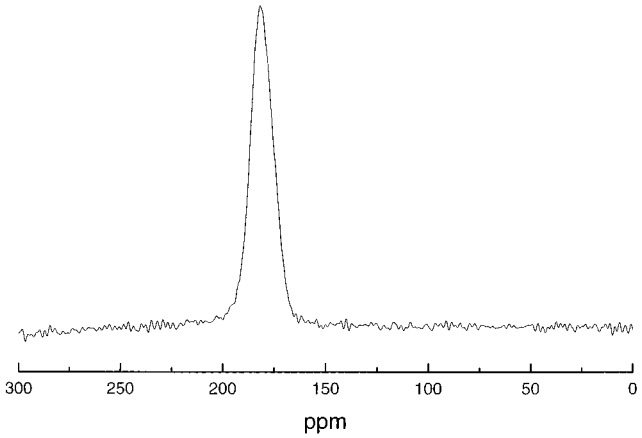

Figure 1. Wideline ^{13}C NMR spectrum of $(ND_3)_8Na_2C_{60}$.

^{2}H NMR Spectroscopy. The ^{2}H wideline solid-state NMR measurements on $(ND_3)_8Na_2C_{60}$ at 150 and 300 K are shown in Figure 2. At 150 K, a Pake doublet pattern is observed, suggestive of an axially symmetric electric field gradient tensor interacting with the quadrupole moment of the ^{2}H nucleus. This demonstrates that the ND_3 molecule has axial symmetry on the NMR time scale. The effective nuclear quadrupole coupling constant at 150 K, given by $4/3\Delta\nu$ where $\Delta\nu$ is the separation between the inner discontinuities of the pattern, is 70.5 ± 0.5 kHz. It is important to note that variable-temperature powder neutron diffraction shows that the space group symmetry is unchanged at this temperature. This is consistent with the molecule undergoing a reorientation about its C_3 axis with a frequency of greater than 10^8 Hz, and an effectively undistorted ammonia geometry ($\Delta\nu$ is 72.5 ± 0.9 kHz in solid ND_3 between 159 and 185 K,[25] and 71.6 ± 0.5 kHz in the $Ag(ND_3)_2^+$ complex at 300 K[25]). At 300 K, a heterogeneity in the characteristic times for reorientation of the ammonia molecules can be observed, with a sharp central peak suggestive of isotropic reorientation of the ammonia molecules. The spectra in the temperature range including 150 and 300 K were modeled by using an isotropic reorientation of the $Na-ND_3$ complex with a variety of activation energies. The quadrupole splitting of the Pake pattern decreases to 65.0 ± 0.5 kHz on warming to

(23) Tycko, R. *J. Phys. Chem. Solids* **1993**, *54*, 1713−1723.

(24) Douthwaite, R. E.; Green, M. L. H.; Rosseinsky, M. J. *J. Chem. Soc., Chem. Commun.* **1994**, 2027−2028.

(25) Rabideau, S. W.; Waldstein, P. *J. Chem. Phys.* **1966**, *45*, 4600.

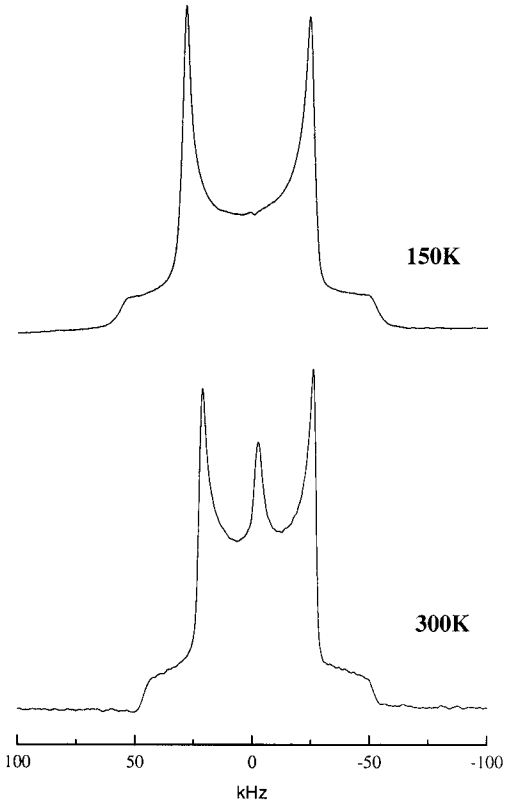

Figure 2. Wideline ^{2}H NMR spectrum of $(ND_3)_8Na_2C_{60}$ at (a) 150 (b) 300 K.

300 K. The axial symmetry of the time-averaged structure is maintained. This implies that any vibration of the C_3 axis has C_3 or greater symmetry: this motion would have an amplitude of 16 ± 2° if it was the only contribution to the reduction in the quadrupole splitting, although some contribution may arise from an alteration of the ammonia geometry through flexing of the apex angle with temperature.

Structure Solution of the Rhombohedral Phase. The volume of the *R*-centered hexagonal cell (2883 Å^3) indicates that it contains three C_{60} molecules. *Ab initio* solution of the structure from both the X-ray and neutron data failed. The strategy adopted was to construct a model based on molecular packing considerations and the available NMR evidence, to explore the effect of the orientations of the molecular species present on the quality of fit and thereby deduce a starting point for final refinement sufficiently close to the global minimum to allow convergence.

A C_{60} molecule at the origin of the rhombohedral cell has six C_{60} nearest neighbors at a chemically reasonable separation of 10.24 Å. The initial structural model then involved placing the molecule in the $m\bar{3}$ symmetry "standard" orientation of the Stephens model[26] for the structure of K_3C_{60} (a molecular 3-fold axis is collinear with the *c*-axis of the hexagonal cell). The other non-hydrogen species in the asymmetric unit were then located by difference Fourier analysis of the X-ray powder histogram, yielding three new positions. Refinement in space group $R\bar{3}m$ showed that these positions were occupied by 10 electron species. The distinction between the isoelectronic Na^+ and NH_3 at this stage was then made on chemical grounds. The sodium cation (Na11) occupied the 6*c* 00*z* site ($z \approx 0.41$). The nitrogen atoms of the ammonia molecules occupy two crystallographically independent sites, N12 at the 6*c* position ($z \approx 0.31$), henceforth referred to as the axial ammonia, and the

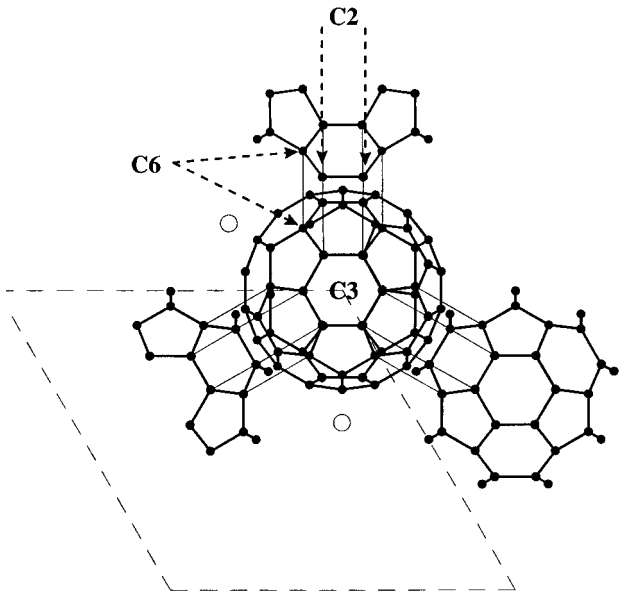

Figure 3. Orientation and interfulleride contacts of the C_{60}^{2-} anions in $(ND_3)_8Na_2C_{60}$. The setting angle of the anion about the hexagonal *c*-axis gives the anion $\bar{3}m$ symmetry, with the mirror planes bisecting the midpoints of the 6:6 bonds in the "polar" hexagon aligned along *c* (generated solely by the C3 carbon). Rotation by 22.24° about *c* generates the $m\bar{3}$ symmetry found in K_3C_{60}. The arrangement of nearest fulleride neighbors is shown in more detail in Figure 8. The present figure shows the mode of interaction between six-membered rings of neighboring C_{60}^{2-} anions. The six hexagons neighboring the polar hexagon directed along the *c*-axis make contact in this way to the six neighboring C_{60}^{2-} anions. The contacts with the three neighbors above the plane of the origin are shown, and involve the C3−C3 6:6 and C3−C6 6:5 bonds on the origin anion and the C6−C2 6:6 and C2−C2 6:5 bonds on the neighbor. The closest C···C approaches discussed in the text are represented by thin solid lines. The axial ammonia is collinear with the *c*-axis and directly above and below the anion at the origin. The equatorial ammonia molecules are located on the mirror planes and represented by the open spheres.

equatorial ammonia N7 on an 18*h* $x\bar{x}z$ position ($x \approx 0.11$ $z \approx 0.44$) (Figure 3). This gives Na···N distances of approximately 2.5 Å in a pseudo-tetrahedral $Na(NH_3)_4^+$ unit. The deuterium atoms were initially located in a series of difference maps calculated from the neutron data. These positions were then used to model the axial and equatorial ammonia molecules in refinements designed to determine the orientation of the fulleride anions.

The molecular symmetry of the C_{60}^{2-} anion was assumed to be $\bar{3}$ and the quality of fit to the neutron data was assessed as the setting angle of the anion about the rhombohedral *c*-axis was increased in 5° steps in the $R\bar{3}m$ and $R\bar{3}$ space groups. The refinements were consistently superior in $R\bar{3}m$. The best model corresponded to a deep minimum in the χ^2(angle) function (8 compared with a maximum value of 160) and involved rotation of between 20 and 25° away from the $m\bar{3}$ starting positions. This angular range contains the rotation angle of 22.24°, which corresponds to the alignment of the molecular mirror planes containing the $\bar{3}$ axis with the $\langle 1\bar{1}0\rangle$ mirror planes of the $R\bar{3}m$ space group,[27] giving $\bar{3}m$ rather than $\bar{3}$ molecular symmetry (Figure 3). This orientation both improves the fit and reduces the number of independent carbon atoms in the asymmetric unit to six. The ordered $R\bar{3}m$ space group was therefore used in the subsequent analysis.

The fit to the neutron data at this stage was unsatisfactory, as the χ^2 of 6.7 was larger than that from a Le Bail intensity

(26) Stephens, P. W.; Mihaly, L.; Lee, P. L.; Whetten, R. L.; Huang, S.-M.; Kaner, R.; Diederich, F.; Holczer, K. *Nature* **1991**, *351*, 632−634.

(27) Burgi, H. B.; Restori, R.; Schwarzenbach, D. *Acta Crystallog.* **1993**, *B49*, 832−838.

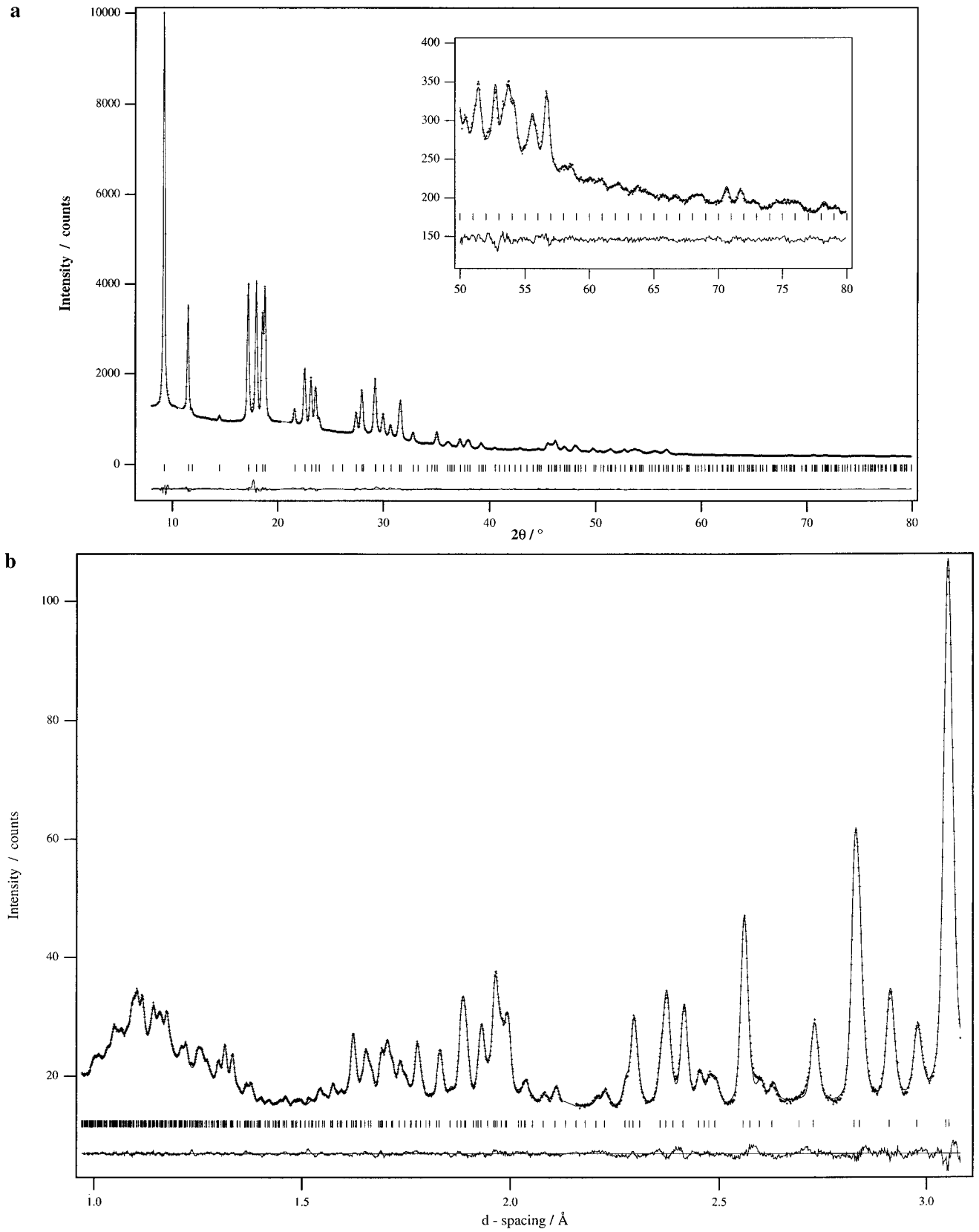

Figure 4. Rietveld refinements of (a) X-ray (the inset shows the high-angle fit) and (b) neutron powder diffraction data on $(ND_3)_8Na_2C_{60}$ at 300 K. The observed data are shown as points, the calculated fit is a solid line, and the difference is given as a continuous curve at the bottom. Ticks mark the locations of the Bragg peaks. The refined parameters are given in Table 1. The agreement indices are $R_{wp} = 1.03\%$, $R_e = 0.56\%$, $R_{F^{**}2} = 1.72\%$ (552 reflections) for the neutron data and $R_{wp} = 1.77\%$, $R_e = 0.85\%$, and $R_{F^{**}2} = 3.71\%$ (275 reflections) for the X-ray data. The final refinement cycles included positional and thermal parameters for all the atoms in the model (T, L tensor elements, rigid body location, orientation angles, and N−D bond length and angle for the equatorial ND_3), without the application of any constraints other than the axial symmetry imposed on the rigid-body ND_3. As all the carbon atoms refined to have identical isotropic temperature factors when refined independently, one isotropic temperature factor was used to describe the thermal motion of the entire anion. Refinement was performed simultaneously against neutron time-of-flight and X-ray histograms collected at 300 K. Goodness of fit to both histograms $\chi^2 = 3.8$ for 3692 observations and 107 variable parameters.

Table 2. Bond Lengths (Å) in the C_{60}^{2-} Fulleride Anion in $(ND_3)_8Na_2C_{60}$ at 298 K[a]

C1−C5 6:6 (×6)	1.379(4)	C2−C2 6:5 (×6)	1.455(4)
C2−C6 6:6 (×12)	1.386(3)	C2−C4 6:5 (×12)	1.472(3)
C3−C3 6:6 (×6)	1.386(4)	C3−C3 6:5 (×6)	1.450(4)
C4−C4 6:6 (×6)	1.400(4)	C3−C6 6:5 (×12)	1.447(3)
C1−C6 6:5 (×12)	1.453(2)	C4−C5 6:5 (×12)	1.454(2)

[a] The numbers following the atom identification indicate the type of bond and the number of equivalent bonds in the molecule. The bond angles are all within 1° of 120° for the hexagons and 108° for the pentagons.

extraction ($\chi^2 = 3.1$),[28] which represents the best possible profile refinement in the chosen space group. A series of Rietveld refinements were then carried out to determine the orientations of the ND_3 molecules located at the axial and equatorial positions. Isotropically disordered models, with the deuteriums located at the vertices of cubes and other Platonic solids, all gave considerably poorer agreement ($\chi^2 = 30$) than models retaining recognizable ND_3 molecules. Refinement indicated 2-fold orientational disorder of both ammonia molecules, as the molecular mirror planes are not aligned with the crystallographic ones. The axial ND_3 molecule was described with one deuterium atom (D13) on a general position, while the equatorial ND_3 was refined as a rigid body, with axial symmetry consistent with the ^2H NMR, and an initial geometry taken from solid ND_3.[29] The location and orientation (defined by the rotation angles about three Cartesian axes) of this group were refined to give $\chi^2 = 3.9$. A search of the rotation space showed the fit to be extremely sensitive to the orientation of the equatorial ND_3, with the freely refined setting angles corresponding to the global minimum orientation (which is defined to ±2° about each axis by the data). Attempts to include other orientations of the equatorial ammonia molecule into the fit failed. The equatorial ammonia orientation and, importantly, its mode of interaction with the neighboring C_{60}^{2-} anions are therefore well-determined in this analysis.

Final refinement cycles involved anisotropic thermal motion of the equatorial ND_3 parametrized with the **TLS** model,[30] using **T** and **L** tensors (the **S** component was statistically insignificant) with symmetry appropriate to the mirror plane location of the nitrogen atom at the center of the rigid body. The rigid body geometry was refined, constrained such that there is one N7−D bond length and one ∠D−N7−D angle. This model refines to $\chi^2 = 3.11$, $R_w = 0.96\%$, and $R_{F^{**}2} = 1.41\%$. The final difference Fourier map had a mean density of less than 0.5% of the strongest peak in the observed map.

This model was then used in a combined refinement of the X-ray and neutron powder diffraction histograms. Inclusion of the X-ray histogram left the ammonia geometry unchanged while improving the estimated standard deviations on the Na−N distances and angles by 100%, reducing the spread in the C−C bond lengths and angles, and halving the deviation of the fulleride anion from spherical symmetry. The sodium site occupancy refines to 100%. We therefore discuss the structure in terms of the parameters and bond lengths derived from the combined refinement (Tables 1−3). The Rietveld fits to the X-ray and neutron data are shown in Figure 4.

Description of the Structure. The structure is shown in Figure 5. The geometry of the C_{60}^{2-} anion (Table 2) proved extremely robust in the refinement, and the anion is very well ordered orientationally. The positional parameters of all six carbon atoms in the asymmetric unit could be refined independently without constraints and did not depend on the models adopted for the axial or equatorial ammonia molecules. The resulting anion is nearly spherical with a mean radius of 3.546(10) Å. This is consistent with expansion with fulleride charge shown by the radii of neutral C_{60} (3.542 Å[31]), C_{60}^{3-} in K_3C_{60} (3.552(9) Å), and C_{60}^{6-} in K_6C_{60} (3.560(8) Å).[32] The mean lengths of the 6:6 and 6:5 bonds at the hexagon−hexagon and hexagon−pentagon junctions are 1.388(6) and 1.456(8) Å, respectively, compared with 1.391(8) and 1.455(8) Å in neutral C_{60} when orientationally ordered[33] and 1.399(2) and 1.446(2) Å in $[PPN^+]_2[C_{60}^{2-}]$.[34]

Table 3. Bond Lengths (Å) and Angles (deg) Within the $Na(ND_3)_4^+$ Complex in $(ND_3)_8Na_2C_{60}$[a]

Na11−N7	2.440(4)	N7−D8	0.927(6)
Na11−N12	2.388(6)	N12−D13	1.032(6)
N7−Na11−N12	103.8(2)	D13−N12−D13	109.9(6)
N7−Na11−N7	114.5(1)	D8−N7−D9	104.3(8)

[a] The atoms N7 and D8−D10 comprise the equatorial ammonia molecule, and N12 and D13 the axial ammonia. The equatorial ND_3 molecule comprising N7, D8, D9, and D10 was constrained to have one N−D bond length and one D−N−D angle.

The refined geometry of the equatorial ammonia (Table 3) is consistent with foreshortening of the N7−D bonds due to the librational motion, with an N7−D bond length of 0.927(6) Å and a bond angle of 104.3(8)° (the largest root mean square libration of 20° will shorten the apparent N−D distance by approximately 0.07 Å, giving a corrected bond length of 0.99 Å). The axially symmetric rigid body description, combined with the anisotropic description of the thermal motion, thus allows a physically sensible model of the ammonia geometry that is capable of accounting for both the symmetry and dynamics of the ammonia molecule apparent in the ^2H NMR. The axial ND_3, whose deuterium atom has a smaller equivalent isotropic temperature factor, has an N−D bond length of 1.032(6) Å and a bond angle of 109.9(6)°. These geometries are consistent with large angle neutron scattering measurements which indicate that the ND_3 geometry is very similar in solid and liquid ND_3 and in the expanded metals $Ca(ND_3)_6$ and $Li(ND_3)_4$, with $r_{ND} = 1.016(4)$ Å and ∠D−N−D = 103.5°.[35]

The $Na(ND_3)_4^+$ complex is shown in Figure 6. The parameters in Table 3 show that it is distorted from tetrahedral symmetry through squashing along the unique axis, which is defined by the Na−N12 vector. The 3-fold axis of the axial ND_3 is collinear with the Na−N12 vector, whereas the molecular 3-fold axis of the equatorial ND_3 makes an angle of 152.6° with the Na−N7 vector.

The closest nonbonded N···D contact is 2.89 Å between N7 and D9, over 0.5 Å longer than the N···D hydrogen bonds in solid ND_3, indicating that coordination of ND_3 to Na^+ prevents the molecules from acting as the donors in intercomplex hydrogen bonds. A similar effect has been noted in the structure of the expanded metal $Li(ND_3)_4$.[36]

(28) Le Bail, A.; Duroy, H.; Fourquet, J. L. *Mater. Res. Bull.* **1988**, *23*, 447.
(29) Hewat, A. W.; Riekel, C. *Acta Crystallogr.* **1978**, *A35*, 569−571.
(30) Schomaker, V.; Trueblood, K. N. *Acta Crystallogr. B* **1968**, *24*, 63.
(31) Chow, P. C.; Jiang, X.; Reiter, G.; Wochner, P.; Moss, S. C.; Axe, J. D.; Hanson, J. C.; McMullan, R. K.; Meng, R. L. *Phys. Rev. Lett.* **1992**, *69*, 2943.
(32) Allen, K. M.; David, W. I. F.; Fox, J. M.; Ibberson, R. M.; Rosseinsky, M. J. *Chem. Mater.* **1995**, *7*, 764−770.
(33) David, W. I. F.; Ibberson, R. M.; Matthewman, J. C.; Prassides, K.; Dennis, T. J. S.; Hare, J. P.; Kroto, H. W.; Taylor, R.; Walton, D. R. M. *Nature* **1991**, *353*, 147.
(34) Paul, P.; Xie, Z.; Bau, R.; Boyd, P. D. W.; Reed, C. A. *J. Am. Chem. Soc.* **1994**, *116*, 4145−4146.
(35) Leclercq, F.; Damay, P.; Chieux, P. *J. Phys. IV* **1991**, *Colloque C5*, 357−363.
(36) Young, V. G.; Glaunsinger, W. S.; von Dreele, R. B. *J. Am. Chem. Soc.* **1989**, *111*, 9260.

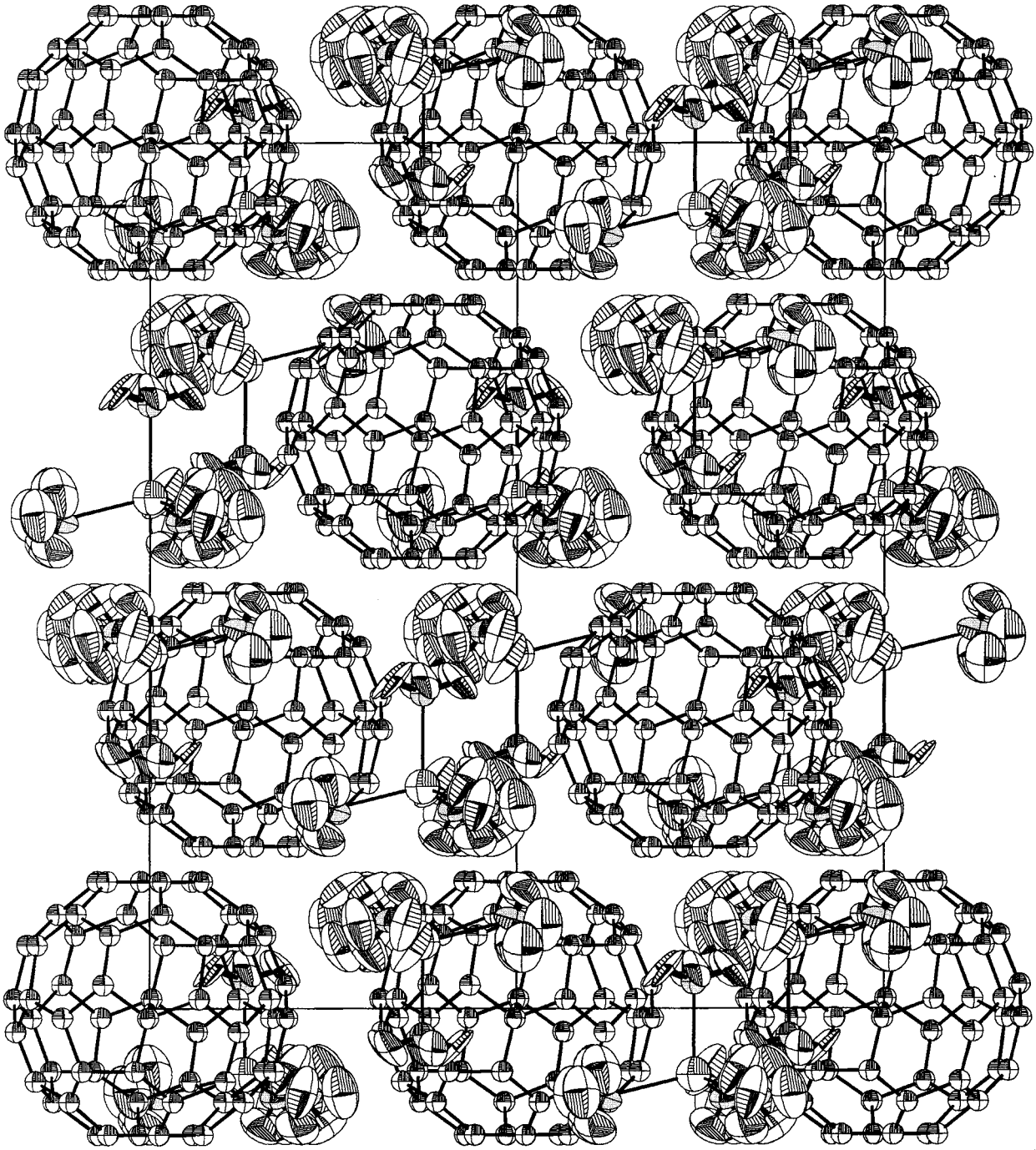

Figure 5. ORTEP representation of the structure of $(ND_3)_8Na_2C_{60}$ at 300 K in space group $R\bar{3}$ viewed along the [110] direction of the *R*-centered hexagonal unit cell. Shown with 40% thermal ellipsoids. The refined structure is in the higher symmetry $R\bar{3}m$ space group, due to positional disorder of the equatorial and axial ammonia molecules over two orientations, which is not shown here for clarity.

Discussion

Na_2C_{60} forms two stable phases with ammonia, pseudo-bcc $Na_2(NH_3)_{5.3}C_{60}$ and a new rhombohedrally packed phase found at higher pressures. The fcc packing of the Na_2C_{60} starting material can be represented as a primitive rhombohedral cell with $a_{rhomb} = r(C_{60}-C_{60}) = 10.0$ Å and $\alpha_{rhomb} = 60°$ or the equivalent *R*-centered hexagonal cell with $a = 10.0$ Å and $c = 24.49$ Å. Each C_{60} has 12 nearest neighbors at the vertices of a cuboctahedron, with six near neighbors in the hexagonal *ab* plane in one close-packed layer and six from the neighboring layers arranged octahedrally, produced by the rhombohedral centering translations (2/3,1/3,1/3) and (1/3,2/3,2/3). This allows the fcc structure to be related to the $a = 12.221$ Å, $c = 22.296$ Å cell ($a = 10.24$ Å, $\alpha = 73.21°$) of $(ND_3)_8Na_2C_{60}$. The six neighboring molecules in the *ab* plane have been displaced to 12.22 Å away. The formerly close packed layers are thus expanded—there are still six neighbors in the layer, but the anions are no longer in contact. The ABCA stacking along the rhombohedral *c*-axis is retained—the now-expanded layers are stacked to maintain the close-packed contacts *between* the layers (Figure 7). This produces a trigonal antiprismatic arrangement of nearest C_{60}^{2-} neighbors at 10.24 Å surrounding each C_{60}^{2-}.

This change in packing appears to be driven by the requirement to coordinate all of the sodium cations equally, and to accommodate the resulting large $Na(ND_3)_4^+$ complexes. The structure can then be thought of as arising from a hierarchy of weak intermolecular interactions, with the coordination of ND_3 to Na^+ dominating to allow the formation of the pseudo-

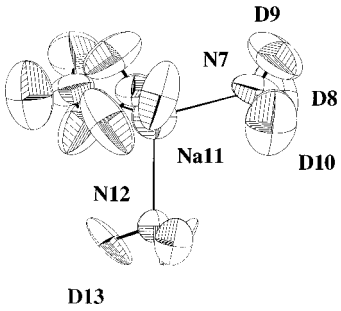

Figure 6. $Na(ND_3)_4^+$ complex from the structure of $(ND_3)_8Na_2C_{60}$ in *R*3 symmetry shown with 50% thermal ellipsoids. The nitrogen atom (N12) from the axial ammonia molecule was refined isotropically.

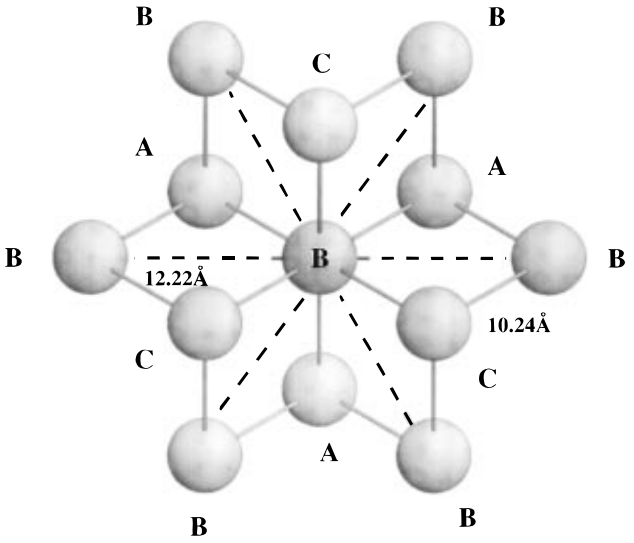

Figure 7. View along the *c*-axis of the *R*-centered hexagonal cell showing the trigonal antiprismatic arrangement of nearest neighbors of each C_{60}^{2-} anion. The 10.24 Å interlayer contacts are shown as hollow lines to the six nearest neighbors: the close contacts to the B layer fulleride ($z = 0$) are to the neighboring A ($z = -1/3$) and C ($z = +1/3$) layers. The six 12.22 Å intralayer nearest neighbor distances within the B layer are coincident with the *a* and *b* cell vectors and represented by the thick dotted lines.

tetrahedral complexes. These groups then control the fulleride packing through the weak C···D interactions. The C···D contacts are the only intermolecular nonbonded distances which are close to or shorter than the sum of van der Waals radii. Both the Na−D10 distance of 2.57(2) Å and the closest C···C nonbonded contacts are 0.4 Å longer than the van der Waals radius sum. An estimate of the sum of the carbon and deuterium van der Waals radii is 2.95 Å,[37] which is also the closest H···C approach in the herringbone packing of benzene.[38]

In Figure 8, the location of the complexes in the ABC stacking sequence of the expanded layers is shown in relation to the octahedral (O) and tetrahedral (T) sites occupied in fcc A_xC_{60} ($x = 1-3$) fullerides. The sodium cation position in $Na_2(ND_3)_8C_{60}$ corresponds to full occupancy of two sites produced by displacement of 1.91 Å away from the center of the octahedral site along the *c* axis. Each C_{60}^{2-} is therefore surrounded by six $Na(ND_3)_4^+$ complexes, three below and three above the fulleride layer. The nitrogen atoms of the axial ammonia molecules in the AB interlayer gap occupy positions displaced toward the B layer by 1.14 Å from the tetrahedral site. This allows coordination to the sodium cation from the octahedral site in the BC gap, which is displaced toward the B layer, and brings the axial ammonia in the AB gap close to the three anions in the B layer which form the basal plane of the original tetrahedral site. The center-to-center separation of the axial ammonia from its fulleride neighbors is 6.74 Å to the apex of the tetrahedron (A layer) and 7.09 Å to the three basal fullerides (B layer).

A conservative interpretation of the structure can now be made in terms of producing contacts of greater than 2.95 Å between D13 from the axial ammonia and the carbon atoms of its four neighboring C_{60}^{2-} anions. The axial ammonia is located directly above the polar hexagon of the apical fulleride, making C···D contacts of 3.178(8) Å to C3 (Figure 9). The *inter*layer $C_{60}-C_{60}$ separation can thus be maintained at 10.24 Å, without generating unfavorable C···D repulsions. Each of the three deuteriums from the axial ND_3 is directed toward one of the three basal C_{60}^{2-} anions in the B layer, located over a five-membered ring of the basal C_{60}. In order to have C···D contacts of longer than 2.95 Å (the closest contact is 3.029(8) Å between D13 and C4) the six *intra*layer interfulleride distances increase to 12.22 Å. The closest D···C contacts between the axial deuterium and the basal fullerides are to the electron-deficient pentagons and therefore likely to derive from repulsion minimization rather than an attractive interaction.

The nonbonded C···D contacts between the C_{60}^{2-} and the equatorial ND_3 groups are considerably shorter than for the axial ammonia because the center-to-center separation is 6.62 Å. The closest C···D contacts are 2.870(8) (D8) and 2.76(1) Å (D10), the latter being significantly shorter than the van der Waals radius sum. The interactions are intriguing, given the recent interest that has been focused on hydrogen bonds of the type X−H···π (X = N, O) where π is an electron-rich system such as alkene, alkyne, or phenyl.[39−41] Each C_{60}^{2-} makes 12 of these closest contacts, to two ND_3 molecules from each neighboring $Na(ND_3)_4^+$ complex, via 12 of its hexagonal rings. These six-rings lie in an equatorial belt below the two polar hexagons directed along *c*, which interact with the axial ammonias, and their six neighboring hexagons which take part in the interfulleride contacts. The deuterium atoms D8 and D10 lie over the centroids of the six-membered rings (Figure 10), with D10−centroid and D8−centroid distances of 2.61(14) and 2.67(21) Å, respectively (the number in brackets represents the displacement from the geometric center of the hexagon in each case). The N7···centroid distance is 3.38 Å, and centroid···D−N7 angles are 142.3° (D10) and 134.9° (D8), compared with average database-derived values for an N−H···phenyl hydrogen bond of 2.47 Å (H···centroid), 3.31 Å, and 148°.[42] The D···centroid distances vary by only 0.08 Å in refinements involving different treatments of the thermal motion and either rigid body or unconstrained refinement of the equatorial ND_3 molecule: the model discussed here is the most conservative in that it yields the longest distances.

The refined structure is therefore suggestive of weak hydrogen bonding between the electron-rich hexagons of the C_{60}^{2-} anions and the deuterium atom of the equatorial ND_3. The appropriate contrast is with the axial ND_3−hexagon interaction, in which none of the C···D contacts are less than the van der Waals radius sum and the D13···centroid and N7···centroid distances are 3.29 and 3.48 Å. The six-membered rings on the fulleride anion

(37) Taylor, R.; Kennard, O. *J. Am. Chem. Soc.* **1982**, *104*, 5063.
(38) Desiraju, G. R.; Gavezzotti, A. *Acta Crystallogr., Sect. B* **1989**, *45*, 473.
(39) Atwood, J. L.; Hamada, F.; Robinson, K. D.; Orr, G. W.; Vincent, R. L. *Nature* **1991**, *349*, 683−684.
(40) Hanton, L. R.; Hunter, C. A.; Purvis, D. H. *J. Chem. Soc., Chem. Commun.* **1992**, 1134−1136.
(41) Allen, F. H.; Howard, J. A. K.; Hoy, V. J.; Desiraju, G. R.; Reddy, D. S.; Wilson, C. C. *J. Am. Chem. Soc.* **1996**, *118*, 4081−4084.
(42) Viswamitra, M. A.; Radhakrishnan, R.; Bandekar, J.; Desiraju, G. R. *J. Am. Chem. Soc.* **1993**, *115*, 4868−4869.

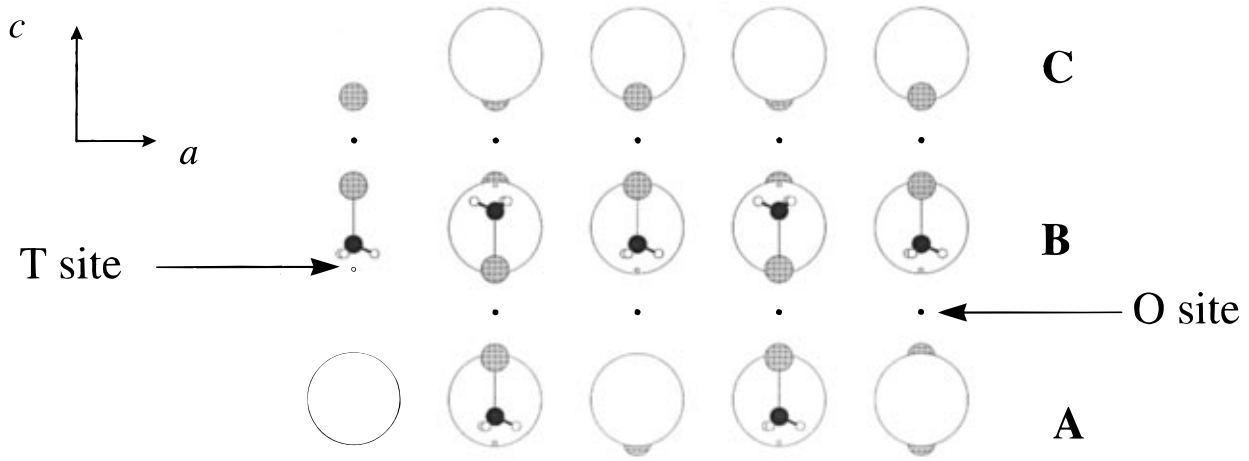

Figure 8. The ABC stacking sequence of expanded fulleride layers in $(ND_3)_8Na_2C_{60}$. The fulleride anions are represented as spheres. The formation of the complex cations is illustrated by depiction of a subset of the axial ammonia molecules and sodium cations. Between two successive fulleride layers (B at $z = 0$ and C at $z = +1/3$), the tetrahedral sites (open small spheres) are at $z = 0.08$, 0.25 and the octahedral site (black small spheres) is at $z = 0.16$. The sodium cations and axial ammonia molecules are seen to be displaced from the tetrahedral and octahedral sites, with an ammonia molecule from the AB gap coordinating a sodium cation in the BC gap.

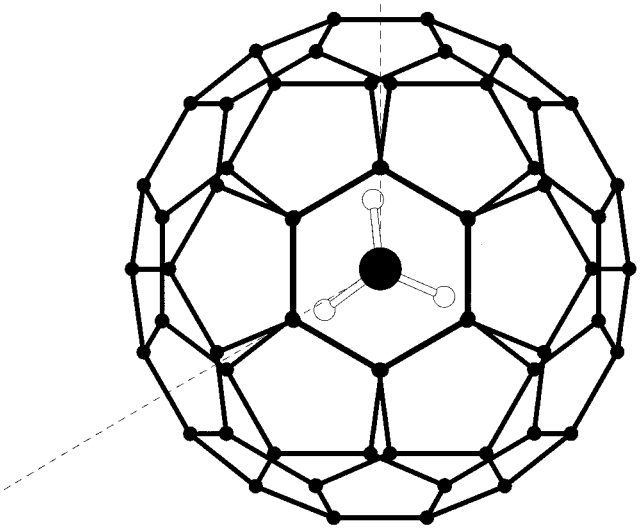

Figure 9. One of the two orientations of the axial ND_3 molecule, showing the closest contacts to the C_{60}^{2-} anion at the apex of the tetrahedral site (in the A layer for the axial ammonia in the AB gap in Figure 8). The second orientation is produced by the mirror planes bisecting the 6:6 bonds of the C_{60}, giving each carbon atom (C3) in the polar hexagon closest to the axial ammonia an equivalent average environment with closest C···D contacts of 3.178(8) and 3.345(8) Å.

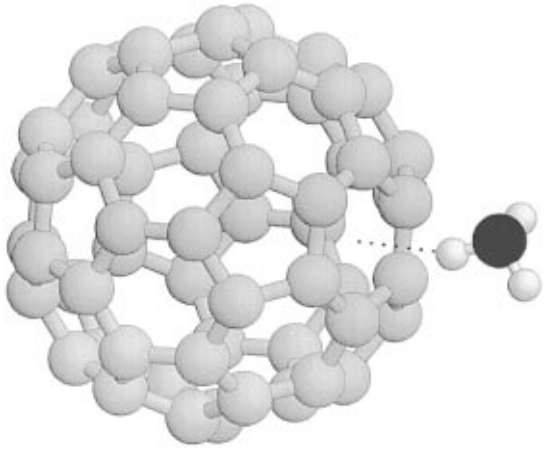

Figure 10. The N−D···π interaction between D10 and a six-membered ring of the C_{60}^{2-} anion.

are able to form these weak interactions because they are relatively electron rich and sterically unhindered. Delocalization of the π electrons over the adjoining pentagons will make the six-membered rings on the surface of the fulleride anion weaker donors than an isolated phenyl group, probably accounting for the slightly longer distances observed here. The ordered 120 K structure of C_{60}·$6SbPh_3$ has a 2.80 Å C−H···hexagon centroid separation, assuming a 0.95 Å C−H bond length.[43]

The N−D···π interactions via D8 and D10 allow each equatorial ammonia to bridge two C_{60}^{2-} neighbors at 12.22 Å in the expanded layers, forming an extended array of weak hydrogen bonds (Figure 11). As the locations of the equatorial ammonia molecules are correlated through complexation to the central Na^+ cation, all the 12.223 Å fulleride neighbors of a given C_{60} are located via the close C···D contacts emanating from the $Na(ND_3)_4^+$ complexes. These interactions reinforce the purely repulsive C···D interactions with the axial ammonia and produce the unusual six plus six "expanded close-packed" environment of the fulleride anion.

The $\bar{3}m$ orientational order of the C_{60}^{2-} anions is determined by the requirement to align the electron-rich six-rings to form the extended array of weak hydrogen bonds with the equatorial ammonia molecules. The closest C···C nonbonded contacts are to the six C_{60} molecules at 10.24 Å in adjacent layers, via the six hexagons neighboring the polar hexagons aligned along the *c*-axis. Each interaction involves close contacts between one six membered ring in each molecule with four 3.74 Å contacts (C2···C3) arising from the alignment of the C3−C3 6:6 bond with the C2−C2 6:5 bond, and two 3.76 Å contacts (C6···C6) from alignment of the C6−C2 6:6 bond with the C3−C6 6:5 bond (Figure 3).

The crystalline rhombohedral phase is accessible via the bcc $n = 5$ phase. Isotropic expansion of the twelve 10.0 Å contacts in Na_2C_{60} to eight nearest neighbors at 10.5 Å, with a volume per C_{60} of 901 $Å^3$ in the $n = 5$ phase, occurs before the increased ammonia loading produces a combination of a further increase in volume per anion to 961 $Å^3$ with a *contraction* in the nearest neighbor distance from the bcc phase to 10.24 Å (six molecules) with six more distant neighbors at 12.22 Å. The closest C···C distances therefore increase despite the overall expansion of the solid, and the retention of a three-dimensional structure.

The ^{13}C and ^{2}H NMR data show that there are complex

(43) Fedurco, M.; Olmstead, M. M.; Fawcett, W. R. *Inorg. Chem.* **1995**, *34*, 390.

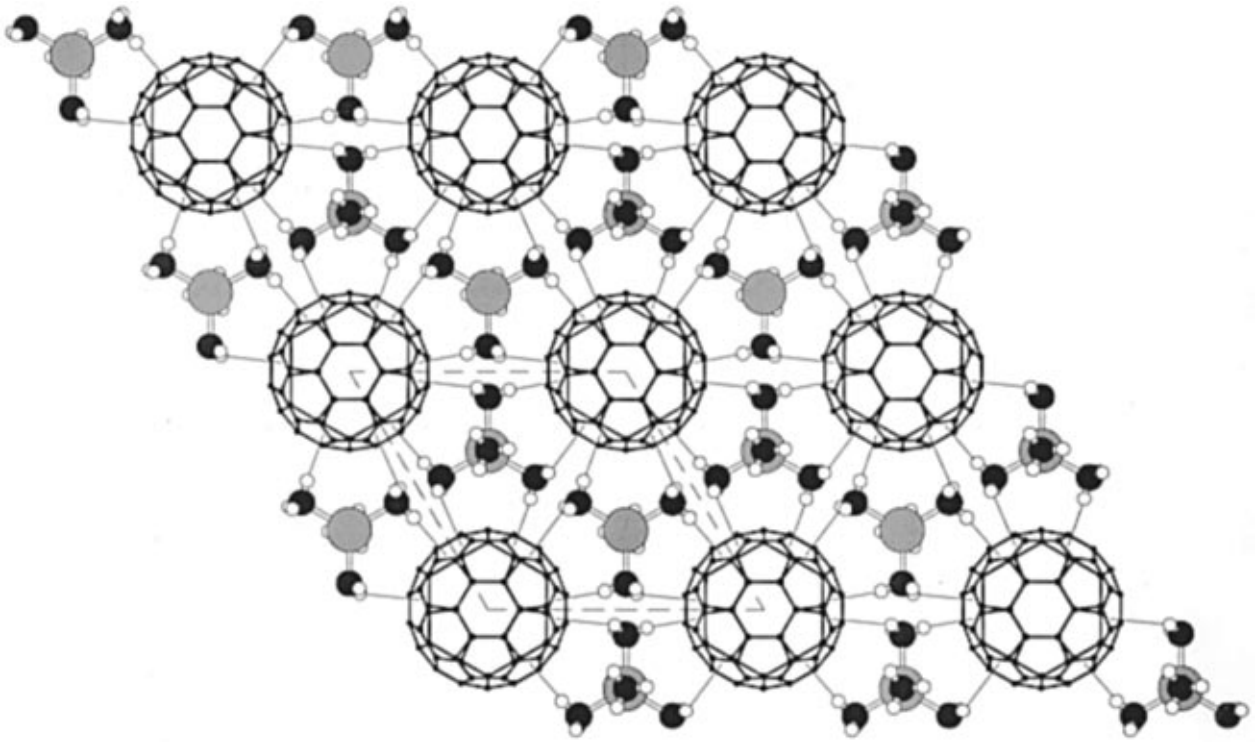

Figure 11. The weak hydrogen bonds between the equatorial ammonia and the fulleride anions form an extended network within the expanded fulleride layers. The thin lines show the hexagon centroid over which the deuterium atoms lie. Each equatorial ammonia molecule interacts via two deuterium atoms with two C_{60}^{2-} anions separated by 12.22 Å. The third deuterium makes contact to a C_{60} in a neighboring layer (not shown) at 10.24 Å from the other two C_{60}^{2-} groups. The sodium cations are shown as gray, and those plotted beneath an axial ammonia molecule lie below the fulleride plane (at $z = -0.08$) while the remaining sodium cations are in the interlayer gap above the plane ($z = +0.08$). The structure is shown with $R\bar{3}$ symmetry and thus only one of the two mirror related orientations of the equatorial ammonia is depicted.

reorientational dynamics within the structure, indicating that the weak C···D interactions are insufficient to prevent ammonia and fulleride motion. At 150 K, both axial and equatorial ammonia molecules are undergoing rapid reorientation about their C_3 axes. At 300 K, the ^{2}H NMR indicates that all the ammonia molecules undergo reorientation about the C_3 axis with a frequency of greater than 10^8 Hz, together with an isotropic reorientation. Detailed analysis of the isotropic central peak is consistent with isotropic reorientation of the ammonia molecules with a distribution of rates, consistent with a spread of activation barriers.[44] The scattering density from both N and D is not spherically disordered on the 10^{-17} s neutron diffraction time scale. The isotropic reorientation cannot then involve tumbling of individual ND_3 molecules about their centers of mass or rotational diffusion of the ND_3 in the complex about the sodium cation, but must involve jump pairwise interchange between axial and equatorial ND_3 molecules.

The heterogeneity of the isotropic reorientation in an apparently well-ordered molecular crystal is surprising. Inspection of the structure indicates that there are two sources for this behavior which may arise either from the existence of different sites with different activation barriers or a distribution of rates within an individual complex. The diffraction data allow a range of statically or dynamically disordered equatorial ammonia orientations (defined within 4° about each Cartesian axis), producing a distribution of local environments in which reorientation of the $Na(ND_3)_4^+$ complex can take place. In addition, the location of the equatorial ND_3 on a mirror plane makes the real $R\bar{3}m$ structure more disordered than the $R\bar{3}$ representation in Figure 11. The existence of two mirror-related orientations of both the axial and equatorial molecules produces a range of local complex symmetries. These will differ from the bulk average refined from the diffraction data when all the equatorial groups in a given complex do not adopt the same orientation, as the 3-fold axis is then lost locally. These sources of local heterogeneity are sufficient to produce the distribution of axial−equatorial and equatorial−equatorial hopping rates of the ammonia molecule within the pseudotetrahedral complex: the ammonia dynamics are thus consistent with the refined ammonia positions. The occurrence of two reorientation mechanisms has precedent in ternary graphite intercalation compounds. In $KC_{24}(ND_3)_{4.3}$,[45] inelastic and quasielastic neutron scattering show rotation of the ammonia about its C_3 axis down to 78 K, with an activation energy of 5 meV, and isotropic tumbling of the entire $(ND_3)_4K^+$ complex is observed at above 200 K.

The ^{13}C NMR spectrum indicates that the fulleride anions are not static on the NMR time scale. The well-defined carbon atom positions show that this molecular motion also involves jumping between symmetry equivalent positions. The close C···D contacts prevent rotational diffusion of the interacting units, but the hindrance potential is sufficiently low to allow jump diffusion between equivalent orientations which is rapid on the NMR time scale.

Conclusion

The controlled low temperature reaction of Na_2C_{60} with ammonia yields a new relative of the close-packed fulleride structures in which the closest interfulleride contacts are not within but between the formerly close-packed layers. The reaction pathway, via an intermediate pseudo-bcc phase, involves an expansion of the volume per C_{60}^{2-} together with a

(44) Heyes, S. J.; Fowkes, A. J.; Fox, J. M.; Rosseinsky, M. J. In preparation.

(45) Zabel, H.; Neumann, D. A. *Can. J. Chem.* **1988**, *66*, 666−671.

shortening of the closest $C_{60}\cdots C_{60}$ contacts. A combination of minimized repulsion with the deuterium atoms of the axial ammonia molecule and weak hydrogen bonds to the equatorial ammonia act cooperatively to expand the intralayer interfulleride separation to 12.22 Å, while maintaining the interlayer distance at 10.24 Å.

Each of the electron-rich six-membered rings of the fulleride anion plays a key role in the intermolecular interactions giving rise to the unique expanded close-packed structure. Twelve equatorial hexagons are involved in the π hydrogen bonding, six take part in the interfulleride interactions with neighboring layers, and the remaining two polar hexagons locate the complexes in the interlayer gaps by interaction with the axial ammonia molecules. The structure demonstrates the variety of weak intermolecular interactions which can be used to control the assembly of new fulleride arrays. The electronic properties of fulleride salts with close inter-C_{60} contacts are very dependent on the anion charge, with both metallic behavior and superconductivity strongly favored at a charge of $3-$.[46] The 10.24 Å interfulleride separation is only slightly greater than that in the superconductor Rb_3C_{60} and will allow significant intermolecular electron hopping. The temperature dependence of the EPR intensity of the rhombohedral phase[47] suggests nonmetallic behavior for this C_{60}^{2-} salt, as found for Na_2C_{60}.[48] The search for C_{60}^{3-} examples of the rhombohedral structure, with its new array of interfulleride contacts, is now an important task.

Acknowledgment. We thank the U. K. EPSRC for a CASE studentship to A.J.F. (sponsored by CCLRC) and an earmarked studentship to P.F.H., for access to the POLARIS instrument and for partial support of consumables costs and the purchase of the powder X-ray diffractometer. We thank the Leverhulme Trust for their support of this work. We thank Dr. M. Hofmann (RAL) for his assistance with the neutron powder diffraction data collection, Dr. M. A. Green (Inorganic Chemistry Laboratory, University of Oxford) for assistance with the BIOSYM software, Professor R. B. von Dreele (Los Alamos National Laboratory) for information on the GSAS programmes, and Dr. D. J. Watkin (Chemical Crystallography Laboratory, University of Oxford) for several helpful discussions concerning TLS matrices.

Supporting Information Available: The ammonia uptake isotherm and the anisotropic temperature factors from the refinement (2 pages). See any current masthead page for ordering and Internet access instructions.

JA972085I

(46) Yildirim, T.; Barbedette, L.; Fischer, J. E.; Lin, C. L.; Robert, J.; Petit, P.; Palstra, T. T. M. *Phys. Rev. Lett.* **1996**, *77*, 167−170.

(47) Allen, K. M.; Fowkes, A. J.; Rosseinsky, M. J. In preparation.

(48) Petit, P.; Robert, J.; Andre, J.-J.; Yildirim, T.; Fischer, J. E. *2nd International Winter School on Electronic Properties of Novel Materials*; Kuzmany, H., Roth, S., Eds.; 1994; pp 478.